Rotational excitation of NS+ by H-2 revisited: A new global potential energy surface and rate coefficients

C. T. Bop, Y. Kalugina, F. Lique

Rotational excitation of NS^+ by H_2 revisited: a new global potential energy surface and rate coefficients

C. T. Bop,[1] Y. Kalugina,[2] and F. Lique[1]
[1)] *Univ Rennes, CNRS, IPR (Institut de Physique de Rennes) - UMR 6251, F-35000 Rennes, France.*
[2)] *Tomsk State University, 36 Lenin Av., 634050, Tomsk, Russia.*

(*Electronic mail: cheikhtidiane.bop@ucad.edu.sn)

(Dated: 10 May 2022)

Due to the lack of specific collisional data, the abundance of NS^+ in cold dense interstellar clouds was determined using collisional rate coefficients of CS as substitute. To better understand the chemistry of sulfur in the interstellar medium, further abundance modeling using the actual NS^+ collisional rate coefficients are needed. For this purpose, we have computed the first full 4D potential energy surface of the NS^+-H_2 van der Waals complex using the explicitly correlated coupled cluster approach with single, double, and non-iterative triple excitation in conjunction with the augmented-correlation consistent-polarized valence triple zeta basis set. The potential energy surface exhibits a global minimum of 848.24 cm^{-1} for a planar configuration of the complex. The long-range interaction energy, described using multipolar moments, is sensitive to the orientation of H_2 up to radial distances of $\sim 50\ a_0$. From this new interaction potential, we derived excitation cross sections, induced by collision with *ortho*- and *para*-H_2, for the 15 low-lying rotational levels of NS^+ using the quantum mechanical close-coupling approach. By thermally averaging these data, we determined downward rate coefficients for temperatures up to 50 K. By comparing them with the previous NS^+-H_2 data, we demonstrated that reduced dimensional approaches are not suited for this system. In addition, we found that the CS collisional data underestimate ours results by up to an order of magnitude. The differences clearly indicate that the abundance of NS^+, in cold dense clouds retrieved from observational spectra, must be reassessed using these new collisional rate coefficients.

I. INTRODUCTION

Recent observations of sulphur-bearing molecules in photodissociation regions (PDR) such as the Horsehead nebula[1] have revived investigations on the interstellar sulphur chemistry, which is still poorly understood. Indeed, in most of the astrophysical environements where S-bearing species are observed, the sum of observed S-species does not account for the sulfur cosmic abundance. The S- reservoir(s) question is still an unresolved important question.

Despite holding a small percentage of the S-budget, NS^+ plays a key role in the of sulphur chemistry. For instance, most of charge exchange and ion-neutral reactions of S-bearing molecules lead to NS^+.[1] In addition, this cation is claimed to be a valuable PDR tracer since it is more abundant in the PDR than in the core of the Horsehead nebula.[1] This enhanced abundance towards the outer layers of the Horsehead nebula is a signature of the dependence of the NS^+ abundance on the external UV field. Moreover, being present at different evolutionary stages of dark molecular clouds, NS^+ is considered as good barometer and thermometer in these regions.[2]

The large variation of the NS/NS^+ abundance ratio observed between cold molecular clouds ($30-50$) and hot cores (>500) suggests that the chemistry underlying the formation and destruction of these species varies from one medium to another.[2] In molecular clouds, NS^+ likely forms from reactions between atomic nitrogen and SO^+/SH^+.[2] In external layers of PDRs, i.e. UV-irradiated regions, S^+ + NH, SH^+ + N and H_2S^+ + N are expected to be the favorite formation routes of NS^+.[1] In addition, charge exchange reactions between NS and C^+/S^+ are less critical in PDRs than in cold molecular clouds.

Therefore, constraining the chemistry of NS and NS^+ in cold molecular clouds and PDRs is crucially needed. For B1b molecular cloud, the chemical model of Cercnicharo et al.[2] reproduced the observed NS/NS^+ abundance ratio within a factor of ~ 2. However, this finding must be treated with caution since the authors highlighted that they used approximate rate coefficients to interpret the observational spectra of NS^+ and NS.

Accurate abundance modeling requires prior determination of collisional rate coefficients. Without these data, local thermodynamic equilibrium (LTE) conditions which are rarely verified in space, would be considered. This approach has led to underestimate the abundance of NS by a factor of $1.5-2.5$.[2] Since collisional rate coefficients of NS and NS^+ were not available in the leterature, Cernicharo et al.[2] used the rate coefficients of CS[3] for both species. They neglected the fine structure of NS and used a scaling factor of 5 to take into account the ionic nature of NS^+.

Since its interstellar detection, NS^+ has become the target of rotational energy transfer studies induced by collisions. Trabelsi et al.[4] reported rate coefficients for the 11 low-lying rotational levels of this cation due to helium-impact for temperatures ranging up to 300 K. The calculations were based on a three dimensional potential energy surface (which was thereafter averaged using the NS^+ ground vibrational wave functions) computed at the explicitly correlated coupled cluster method with single, double and non-iterative triple excitation in conjunction with the augmented-correlation consistent-polarized valence triple zeta basis (hereafter denoted as CCSD(T)-F12/aug-cc-pVTZ). Few months later, Cabrera et al.[5] used a CCSD(T)/aug-cc-pV5Z 3D PES (a similar accuracy to the PES mentioned above) to revisit the NS^+-He col-

lisional system. They extended the rotational basis up to the 27 low-lying energy levels and resolved the hyperfine structure since such emission lines were also reported.[2] Both authors compared their results with the collisional rate coefficients of CS-He[3] used in the NS^+ abundance modeling. Despite the similarity of their data, Trabelsi et al.[4] validated the use of CS as template for NS^+ while Cabrera et al.[5] highlighted the limits of such an approximation.

Due to the fact that He is seen as a bad template for *para*-H_2 (p-H_2) in the case of charged species, Bop[6] reassessed the hyperfine rate coefficients corresponding to the 23 low-lying rotational levels of NS^+ for temperatures up to 100 K, but using p-$H_2(j_2 = 0)$ as projectile. These calculations were based on a 4D PES, computed at the CCSD(T)-F12/aug-cc-pVTZ level of theory, which was thereafter averaged over the orientations of H_2 (denoted hereafter as model treatment). The comparison with the previous rate coefficients of NS^+ led to deviations of $2-4$ depending on the transition and on the temperature.

The strong anisotropy of the PES of NO^+-H_2,[7] an isoelectronic analogue of NS^+-H_2, with respect to the orientations of H_2 let us reconsider the use of an average potential for the scattering of NS^+ with H_2. In practice, we revisited the scattering of NS^+ due to p-H_2 impact using a full dimensional PES. Since this molecular cation was also observed towards warm/hot environments such as the Horsehead nebula,[1] where the *ortho-to-para*-H_2 ratio is not negligible, rate coefficients by collision with both *ortho*-H_2 (o-H_2) and p-H_2 are needed.

This paper is structured as follows: the computational details are briefly given in Section II, the results are shown and discussed in Section III and concluding remarks are displayed in Section IV.

II. COMPUTATIONAL DETAILS

A. Potential energy surface and analytical fit

The potential underlying the interaction between $NS^+(^1\Sigma^+)$ and $H_2(^1\Sigma_g^+)$, in their ground electronic state, was calculated using the Jacobi coordinate system. The PES was calculated under the assumption of rigid rotor-rigid rotor interaction using the bond lengths averaged with the ground vibrational wave functions, $<r_{H_2}>_0 = 1.449\ a_0$ and $<r_{NS^+}>_0 = 2.7189\ a_0$.[2,8] In practice, 4 degrees of freedom are needed to describe the geometry of the collision complex (see Fig. 1): the intermolecular distance (R), the polar angles of NS^+ and H_2 relative to the **R** vector (θ_{NS^+} and θ_{H_2}, respectively) and the dihedral angle between the half-planes that contain NS^+ and H_2 (ϕ).

In this work, we used as Bop[6] the state-of-the art CCSD(T)-F12/aug-cc-pVTZ level of theory[9,10] implemented in the `MOLPRO` molecular package version 2010[11] for all *ab initio* calculations. We improved the PES Bop[6] by (*i*) fully describing the H_2 rotations and (*ii*) explicitly treating the long-range interaction potential using a multipolar expansion. In fact, the previous PES of the NS^+-H_2 complex was averaged over 3 H_2 rotations : $(\theta_{H_2}, \phi) = (0, 0)$, $(90, 0)$ and $(90, 90)$.[6]

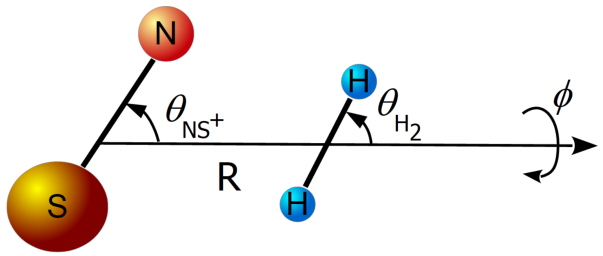

FIG. 1. Coordinate system of NS^+-H_2 complex.

TABLE I. Electric properties of the NS^+ and H_2 monomers computed at the CCSD(T)/aug-cc-pVTZ level of theory. All values are in a. u.

Param.	Definition	NS^+	H_2
μ_z	dipole moment	-0.7805	0.
Θ_{zz}	quadrupole moment	1.0029	0.4866
Ω_{zzz}	octupole moment	-0.7002	0.0
Φ_{zzzz}	hexadecapole moment	-7.79	0.36
Φ_{xxxx}		-2.92	0.14
α_{xx}	dipole polarizability	13.8399	4.7608
α_{zz}		23.4455	6.7291

The basis set superposition error correction was taken into account using the counterpoise method.[12]

The interaction energy $V(R, \theta_{NS^+}, \theta_{H_2}, \phi)$ was expanded in bispherical harmonics $A_{L_1L_2L}(\theta_{NS^+}, \theta_{H_2}, \phi)$:

$$A_{L_1L_2L}(\theta_{NS^+}, \theta_{H_2}, \phi) = \sqrt{\frac{2L_1+1}{4\pi}}\Big[\begin{pmatrix} L_1 & L_2 & L \\ 0 & 0 & 0 \end{pmatrix} \times P_{L_10}(\theta_{NS^+})P_{L_20}(\theta_{H_2}) + 2\sum_{M=1}^{\min(L_1,L_2)} \begin{pmatrix} L_1 & L_2 & L \\ M & -M & 0 \end{pmatrix} \times P_{L_1M}(\theta_{NS^+})P_{L_2M}(\theta_{H_2})cos(M\phi)\Big] \quad (1)$$

where $L = |L_1 - L_2|, ..., L_1 + L_2$, L_1 and L_2 are associated with the rotational motion of NS^+ and H_2, respectively and M is related to the dihedral angle ϕ. Due to homonuclearity of H_2, the index L_2 takes only even values. P_{LM} is the associated Legendre polynomial. The potential in this coupled basis has the following form:

$$V(R, \theta_{NS^+}, \theta_{H_2}, \phi) = \sum_{L_1L_2L} v_{L_1L_2L}(R) A_{L_1L_2L}(\theta_{NS^+}, \theta_{H_2}, \phi). \quad (2)$$

The expansion coefficients $v_{L_1L_2L}(R)$ at each point R (31 R-grid points from 4.5 to 29 a_0) were obtained using 11-point (5-point) Gauss-Legendre quadrature for θ_{NS^+} (θ_{H_2}) and 9 Gauss-Chebyshev quadrature for ϕ. Angles, θ_{NS^+}, θ_{H_2} and ϕ were set to [11.98, 27.49, 43.10, 58.73, 74.36, 90.00, 105.64, 121.27, 136.90, 152.51, 168.02], [13.12, 30.11, 47.20, 64.32, 81.44] and [10, 30, 50, 70, 90, 110, 130, 150, 170], respectively. The use of these quadrature allows us to expand the potential in the coupled basis with $L_1^{max} = 10$ and $L_2^{max} = 6$ which gives us a total of 142 radial expansion coefficients $v_{L_1L_2L}(R)$.

The long-range part of the potential can be represented using analytical multipolar expansion through the order of R^{-6}.[13]

$$V(R,\theta_{NS^+},\theta_{H_2},\phi) = \frac{1}{3}T_{\alpha\beta}q^A\Theta^B_{\alpha\beta} + \frac{1}{105}T_{\alpha\beta\gamma\delta}q^A\Phi^B_{\alpha\beta\gamma\delta} - \frac{1}{2}T_\alpha T_\beta (q^A)^2\alpha^B_{\alpha\beta} + T_\alpha T_{\beta\gamma}q^A\alpha^B_{\alpha\beta}\mu^A_\gamma - \frac{1}{2}T_{\alpha\gamma}T_{\beta\delta}\alpha^B_{\alpha\beta}\mu^A_\gamma\mu^A_\delta - \frac{1}{3}T_{\alpha\beta\gamma}\Theta^B_{\alpha\beta}\mu^A_\gamma + \frac{1}{9}T_{\alpha\beta\gamma\delta}\Theta^B_{\alpha\beta}\Theta^A_{\gamma\delta} - \frac{1}{45}T_{\alpha\beta\gamma\delta\varepsilon}\Theta^B_{\alpha\beta}\Omega^A_{\gamma\delta\varepsilon} - \frac{C^0_6}{6\alpha^A\alpha^B}T_{\alpha\beta}T_{\gamma\delta}\alpha^A_{\alpha\gamma}\alpha^B_{\beta\delta}, \quad (3)$$

In practice, 100 Gauss-Legendre quadrature nodes are considered to determine the isotropic term, $C^0_6 = 40.3027\ E_h a_0^6$, using the (equation-of-motion) EOM-CCSD method[14] implemented in MOLPRO. The average polarizability α and the tensor $T_{\alpha\beta\gamma\ldots\nu}$ are defined as $1/3(\alpha_{xx}+\alpha_{yy}+\alpha_{zz})$ and $\nabla_\alpha\nabla_\beta\nabla_\gamma\ldots\nabla_\nu R^{-1}$, respectively. Superscrips A and B denote molecules NS^+ and H_2, respectively. We implied in Eq. 3 the dependence of multipole moments and polarizabilities of molecule A on angle θ_{NS^+} and of molecule B on angles θ_{H_2} and ϕ. The values of multipole moments and polarizabilities used in analytical calculations are presented in Table I. These values were calculated at the CCSD(T)/aug-cc-pVTZ level of theory using finite-field method.[15]

We noticed that for very large intermolecular separations, CCSD(T)-F12a method started to deviate from the analytical long-range approximation. Therefore, we performed further calculations using standard CCSD(T) along with the aug-cc-pVTZ basis set. Indeed, at intermediate distances $R = 20-22\ a_0$, the CCSD(T) and CCSD(T)-F12a computed energies agree very well whereas discrepancies occur at $R > 29\ a_0$. Using the long-range analytical potential as reference at $R = 100\ a_0$, we obtained slight deviations of $\sim 10^{-5}$% for standard CCSD(T) whereas CCSD(T)-F12a leads to relative errors of up to 30%. In fact, the agreement with CCSD(T) is not surprising since the multipole moments and polarizabilities of monomers (Eq. 3) are computed at the same level of theory. Therefore, to obtain a smooth and accurate interaction potential, we used CCSD(T)-F12a for $R \leq 20\ a_0$, CCSD(T) for $20 < R \leq 25\ a_0$ and the analytical multipolar expansion for $R > 25\ a_0$.

The root-mean-square error (rmse) of the analytical fit (Eq. 2) is about $[10^{-4}-10^{-3}]$ cm^{-1} and $[10^{-2}-10^{-1}]$ cm^{-1} in the attractive and repulsive regions, respectivly. The expansion coefficients obtained from the fit, i.e. for $4.5 \leq R \leq 29\ a_0$, were interpolated using cubic spline routine. For $R > 29\ a_0$, the potential is represented solely by analytical long-range multipolar expansion.

B. Cross sections and rate coefficients

The scattering processes we are studying can be summarised as follows:

$$NS^+(j_1) + o-;p-H_2(j_2) \rightarrow NS^+(j_1') + o-;p-H_2(j_2) \quad (4)$$

where j_1 and j_2 are the NS^+ and H_2 rotational quantum numbers, respectively. The hyperfine structure due to the nuclear spin of nitrogen is not considered in this work but it can be derived from our data using the Infinite Order Sudden (IOS) approximation.[16,17] The cross sections (σ) were calculated for the 15 low-lying rotational levels of NS^+ ($j_1 = 0-14$) for total energies ranging up to at least 500 cm^{-1}. The energy range was spanned using a fine step size of 0.1 cm^{-1} to correctly describe the resonances.

We used the close-coupling quantum mechanical approach[18] implemented in the MOLSCAT code.[19] The log derivative-airy propagator was used to solve the coupled equations.[20] Preliminary test calculations were performed to set the integration parameters. For NS^+, we considered a quite wide rotational basis which includes at least 10 channels above the considered rotational energy levels. Typically, the size of the basis was varied from 23 to 30 rotational levels ($j_1 = 22-29$).

Regarding the H_2 rotational basis, only $j_2 = 0$ and $j_2 = 1$ were used for p- and o-H_2 colliders, respectively. For p-H_2, convergence was checked by comparing the sum of partial cross sections, $\sigma(j_2 = 0)$ and $\sigma(j_2 = 0-2)$, over the 11 first total angular momenta ($J = 0-10$). For total energies of 100 cm^{-1}, 250 cm^{-1} and 500 cm^{-1}, the deviation of $\sigma(j_2 = 0)$ with respect to $\sigma(j_2 = 0-2)$ is less than 30%. In the case of o-H_2, we calculated partial cross sections $\sigma(j_2 = 1)$ and $\sigma(j_2 = 1-3)$ up to $J = 5$ to reduce the computational cost due to the inclusion of $j_2 = 3$. As shown for HCCNC and HNCCC,[21] the more total angular momentum we use, the better the convergence would be. Since the first rotational energy level of H_2 is shifted to ~ 120 cm^{-1} above the ground level, we used total energies of 220 cm^{-1}, 370 cm^{-1} and 620 cm^{-1}. The disagreement between $\sigma(j_2 = 1)$ and $\sigma(j_2 = 1-3)$ is less than 20% except at low energy. For a better appreciation of the convergence, we show in Table II the variation of cross sections as a function of the increment of the H_2 rotational manifold.

The STEPS-parameter was varied from 60 to 10 to keep the integration step small enough. The rotational energy levels were constructed using the spectroscopic constants of NS^+ [$B_0 = 0.835$ cm^{-1} and $D_0 = 1.17\times10^{-7}$ cm^{-1}] and H_2 [$B_0 = 59.322$ cm^{-1} and $D_0 = 0.047$ cm^{-1}].[2,8]

By thermally averaging the so-calculated cross sections over the Maxwell-Boltzmann velocity distribution, we derived collisional rate coefficients (k) for temperatures up to 50 K,

$$k_{j_1,j_2\rightarrow j_1',j_2}(T) = \left(\frac{8}{\pi\mu\beta}\right)^{1/2}\beta^2 \int_0^\infty E_k\sigma_{j_1,j_2\rightarrow j_1',j_2}(E_k)e^{-\beta E_k}\,dE_k \quad (5)$$

where E_k is the kinetic energy, $\mu = 1.931$ au is the reduced mass of the complex and β the inverse of the Boltzmann constant multiplied by the temperature.

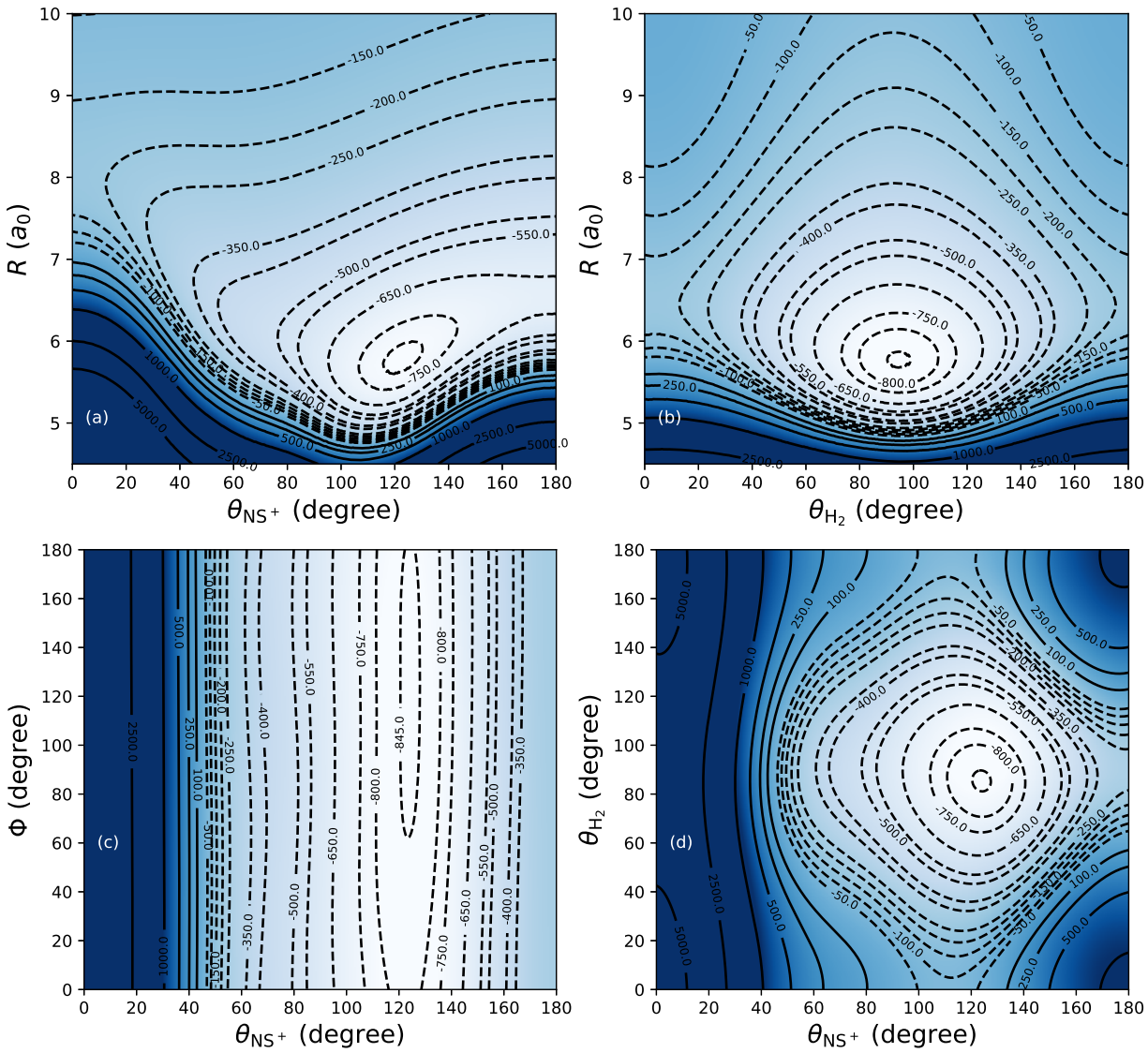

FIG. 2. Contour plots of 2D cuts of the NS^+-H_2 4D PES. The panels (a), (b), (c) and (d) show $V(R, \theta_{NS^+}, \theta_{H_2} = 81.8°, \Phi = 180°)$, $V(R, \theta_{H_2}, \theta_{NS^+} = 124.3°, \Phi = 180°)$, $V(\theta_{NS^+}, \Phi, R = 5.77\ a_0, \theta_{H_2} = 81.8°)$ and $V(\theta_{NS^+}, \theta_{H_2}, R = 5.77\ a_0, \Phi = 180°)$, respectively.

TABLE II. The variation of cross sections ($\mathring{A}^2$) as a function of the increment of the H_2 rotational manifold. For p-H_2 and o-H_2, we summed partial cross sections over the 11 ($J = 0-10$) and 6 ($J = 0-5$) first total angular momenta, respectively.

		p-H_2						o-H_2					
		$E = 100$ cm^{-1}		$E = 250$ cm^{-1}		$E = 500$ cm^{-1}		$E = 220$ cm^{-1}		$E = 370$ cm^{-1}		$E = 620$ cm^{-1}	
j_1	j_1'	$j_2 = 0$	$j_2 = 0-2$	$j_2 = 0$	$j_2 = 0-2$	$j_2 = 0$	$j_2 = 0-2$	$j_2 = 1$	$j_2 = 1-3$	$j_2 = 1$	$j_2 = 1-3$	$j_2 = 1$	$j_2 = 1-3$
1	0	4.01×10^{-1}	5.20×10^{-1}	1.03×10^{-1}	1.38×10^{-1}	6.72×10^{-2}	6.02×10^{-2}	4.16×10^{-1}	5.85×10^{-1}	9.76×10^{-2}	9.20×10^{-2}	4.14×10^{-2}	4.87×10^{-2}
3	2	2.54	2.93	5.08×10^{-1}	6.05×10^{-1}	1.83×10^{-1}	1.85×10^{-1}	9.45×10^{-1}	9.82×10^{-1}	1.74×10^{-1}	1.69×10^{-1}	6.22×10^{-2}	6.44×10^{-2}
7	5	5.73	5.48	8.14×10^{-1}	7.55×10^{-1}	2.09×10^{-1}	1.67×10^{-1}	1.08	1.19	2.23×10^{-1}	2.26×10^{-1}	5.52×10^{-2}	5.54×10^{-2}
9	7	1.11×10^{1}	1.12×10^{1}	9.55×10^{-1}	9.52×10^{-1}	2.27×10^{-1}	2.34×10^{-1}	1.16	1.29	1.83×10^{-1}	1.97×10^{-1}	4.48×10^{-2}	4.75×10^{-2}

III. RESULTS

We display in Fig. 2 bi-dimensional cuts of the 4D PES of the NS^+–H_2 complex through the global minimum (see below). The potential exhibits a strong anisotropy except in panel (c) where it depends weakly on ϕ. The global minimum corresponds to a planar structure where the axes of the H_2 and NS^+ molecules form an acute angle. Typically, we obtained $\theta_{NS^+} = 124.3°$, $\theta_{H_2} = 81.8°$, $\phi = 180.0°$ and $R = 5.77\ a_0$ with ΔE = -849.88 cm^{-1}.

The potential well depth is thus similar to that of Bop[6] which is located at -848.24 cm^{-1} below the dissociation limit

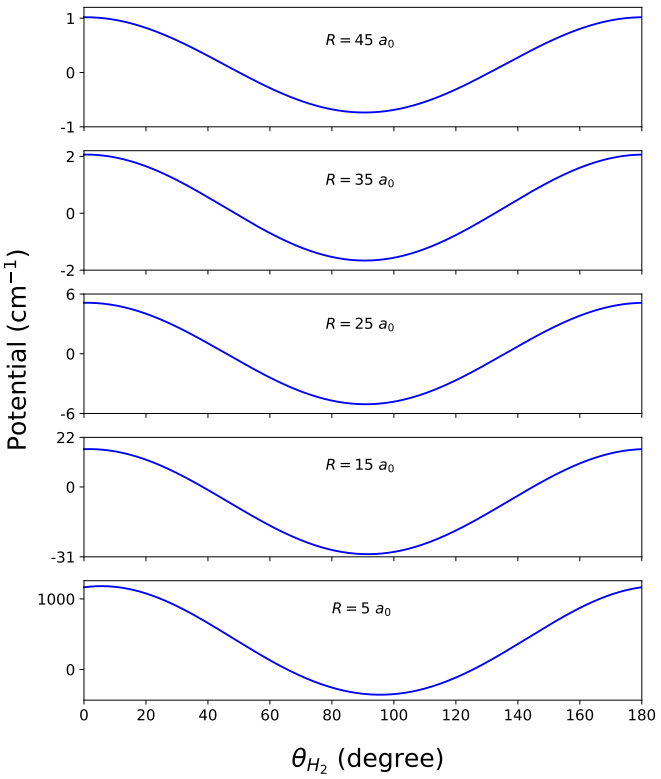

FIG. 3. The dependence of the potential energy with respect to θ_{H_2} at various radial distances. The angles θ_{NS^+} and ϕ are fixed at 124.3° and 180°, respectively.

of the complex. With respect to the interaction potentials where helium was used as projectile,[4,5] the new global minimum is about 5 times deeper.

We plot in Fig. 3 the variation of the potential as a function of θ_{H_2} at various radial distances. As one can see, the PES remains sensitive to the H_2 orientations at long-range. For example at $R = 45\ a_0$, the potential varies by nearly 2 cm^{-1}. In fact the long-range is led by charge-quadrupole interactions which slowly decay as R^{-3} and sensitive to the orientation of the quadrupole, i.e. H_2. In contrast, we notice very slight variations of the PES relative to θ_{NS^+} for $R > 20\ a_0$. This comes from the fact that, charge-quadrupole interactions do not depend on θ_{NS^+} at long-range and the other higher-order interactions (dipole-quadrupole and quadrupole-quadrupole) remain weak relative to charge-quadrupole.

We show in Fig. 4 the variation of the rotational cross sections of NS^+ in collision with both *o*- and *p*-H_2 as a function of the kinetic energy. The amplitude quickly drops with increasing kinetic energy-logarithm, exhibiting the so-called Langevin behaviour which is known for ion-molecule collisional cross sections. In fact, for ion-molecule collisional systems, the cross sections are inversely proportional to the square root of the collision energy. Moreover, both projectiles lead to very close cross sections with slight deviations below 10 cm^{-1}. This behavior is a typical feature of molecular ions.[22] Compared to the previous calculations of Bop,[6] the

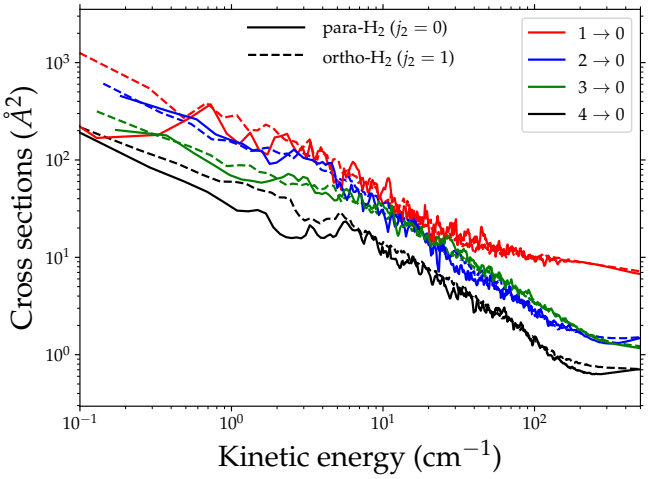

FIG. 4. Variation of the rotational cross sections of NS^+ induced by collision with *o*- and *p*-$H_2(j_2 = 0)$ as a function of the kinetic energy for selected transitions.

shape of the cross sections does not change significantly.

For a better assessment of the improvements we carried on the potential, we show in Fig. 5 a systematic comparison of the NS^+ rotational cross sections induced by *p*-H_2 computed in this work and those reported by Bop[6] at 100 cm^{-1}, 250 cm^{-1} and 500 cm^{-1}. The cross sections derived from the full 4D PES agree mostly within a factor of 2 with the data mentioned above. A comparison using a full energy range would show even more discrepancies than the few points seen in the top panel of Fig. 5. Indeed, the use of two different PESs will lead to a shift of the locations of the resonances, i.e. at low kinetic energy, where the cross sections are very sensitive to the PES. However, it is worth noting that the differences obtained are surprising since reasonable agreement are usually found between full and reduced dimensional approaches for collisions involving ions.[23,24]

To figure out the origin of these discrepancies, we averaged the new potential over the H_2 rotation (i.e. $(\theta_{H_2}, \phi) = (0, 0)$, (90, 0) and (90, 90) as previously done by Bop.[6] The bottom panel of Fig. 5 shows a perfect agreement clearing out any suspicion on the different coordinate systems used in the construction of the PESs. From this comparison, we show the need for PESs describing all the orientations of H_2 in the case of strongly anisotropic interactions.

To settle upon the ambiguity highlighted in the introduction, i.e. whether CS is a good template for NS^+ or not, we compare in Fig. 6 our new collisional data obtained for the *p*-H_2 collider to the CS-He rate coefficients.[25] Despite being scaled up by a factor of 5, the CS-He rate coefficients[25] underestimates the $NS^+ - p$-H_2 ones by nearly an order of magnitude for most transitions. The discrepancy is even greater at 10 K, i.e. the typical temperature of cold media where NS^+ was observed.[2] These strong deviations are not surprising since scaling up rate coefficients of the neutral CS molecule cannot efficiently incorporate the ionic nature of the NS^+ cation, i.e. the Langevin behavior seen in the cross sections. Besides the different shapes, Fig. 6 shows that a factor of at least

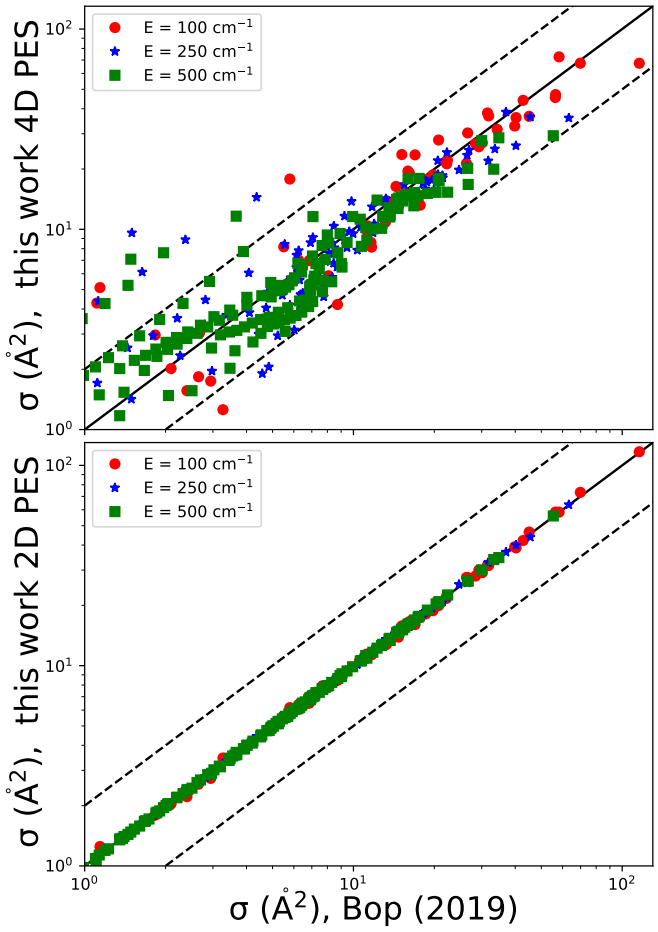

FIG. 5. Systematic comparison of rotational cross sections of NS^+ induced by collision with p-$H_2(j_2 = 0)$ for selected total energies. The data represented in the y-axis are computed using the full 4D PES (top panel) and average 2D PES based on 3 orientations of H_2 (bottom panel). The dashed lines delimit the region where the two sets of data differ by less than a factor of 2.

10 would have been needed to describe reasonably the dominant rate coefficients ($k > 10^{-11}$ cm^3 s^{-1}). The need of such a high multiplier is directly related to the interaction potentials. In fact, the CS-He potential[25] has a well depth of ~ 22 cm^{-1} which is very small compared to that of NS^+-H_2 (~ 850 cm^{-1}).

IV. CONCLUSION

The first 4D PES of the NS^+-H_2 van der Waals complex was calculated using the CCSD(T)-F12/aug-cc-pVTZ level of theory. The long-range interaction was explicitly described using analytical multipolar expansion. Rotational cross sections of NS^+ induced by collision with *ortho*-H_2 ($j_2 = 1$) and *para*-H_2 ($j_2 = 0$) were derived, for total energies up to at least 500 cm^{-1}, using the close-coupling approach. We considered transitions between the 15 low-lying rotational energy levels and we retrieved downward rate coefficients, for temperatures

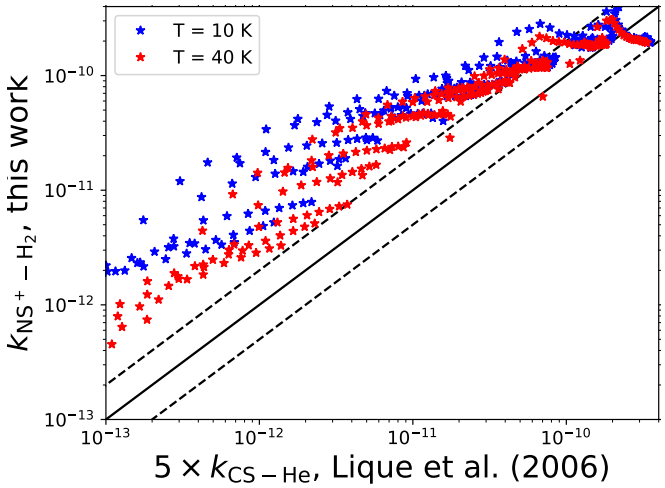

FIG. 6. Systematic comparison of rotational rate coefficients (in cm^3 s^{-1}) for selected temperatures. The x-axis shows the CS-He collisional rate coefficients scaled by a factor of 5 and the y-axis represents the NS^+-p-H_2 data. The dashed lines delimit the region where the agreement is better than a factor of 2.

up to 50 K, by thermally averaging the cross sections.

The collision data obtained using *ortho*-H_2 ($j_2 = 1$) and *para*-H_2 ($j_2 = 0$) as projectiles are very similar suggesting the possibility of using only p-H2 collisional data in radiative transfer calculations. The explicit description of the anisotropy of the PES with respect to the orientations of H_2 led to deviations of a factor of 2 in the cross sections. Concerning the use of CS as template for NS^+, we showed that a scaling factor cannot incorporate the ionic nature.

The data presented in this work, supplemented by the NS-He rate coefficients briefly described in the recent paper of Hily-Blant et al.,[26] will be of great importance to better constrain the evolution of the NS^+/NS abundance ratio in cold dense clouds.

CONFLICTS OF INTEREST

There are no conflicts of interest to declare.

SUPPLEMENTARY MATERIAL

A Fortran routine for generating the potential is available as supplementary material.

DATA AVAILABILITY

The data underlying this manuscript are available from the corresponding author upon reasonable request.

ACKNOWLEDGEMENTS

The authors acknowledge the European Research Council (ERC) for funding the COLLEXISM project, the Programme National "Physique et Chimie du Milieu Interstellaire" (PCMI) of Centre National de la Recherche Scientifique (CNRS)/Institut National des Sciences de l'Univers (INSU) with Institut de Chimie (INC)/Institut de Physique (INP) cofunded by Commissariat a l'Energie Atomique (CEA) and Centre National d'Etudes Spatiales (CNES). F.L. acknowledges the Institut Universitaire de France. Results of ab initio calculations and the fit of the PES have been obtained under support of the RSF grant No. 17-12-01395.

[1] P. Rivière-Marichalar, A. Fuente, J. R. Goicoechea, J. Pety, R. Le Gal, P. Gratier, V. Guzmán, E. Roueff, J. Loison, V. Wakelam, *et al.*, Astronomy & Astrophysics **628**, A16 (2019).
[2] J. Cernicharo, B. Lefloch, M. Agúndez, S. Bailleux, L. Margulès, E. Roueff, R. Bachiller, N. Marcelino, B. Tercero, C. Vastel, *et al.*, The Astrophysical journal letters **853**, L22 (2018).
[3] F. Lique and A. Spielfiedel, Astronomy & Astrophysics **462**, 1179–1185 (2007).
[4] T. Trabelsi, Y. Ajili, K. Hammami, M. Mogren Al Mogren, J. Francisco, and M. Hochlaf, Monthly Notices of the Royal Astronomical Society **480**, 4259–4264 (2018).
[5] L. Cabrera-González, R. Mera-Adasme, D. Páez-Hernández, and O. Denis-Alpizar, Monthly Notices of the Royal Astronomical Society **480**, 4969–4973 (2018).
[6] C. T. Bop, Monthly Notices of the Royal Astronomical Society **487**, 5685–5691 (2019).
[7] C. Orek, M. Umiński, J. Kłos, F. Lique, P. S. Zuchowski, and N. Bulut, Chemical Physics Letters **771**, 138511 (2021).
[8] K. Huber, (Springer US, 2013).
[9] G. Knizia, T. B. Adler, and H.-J. Werner, The Journal of Chemical Physics **130**, 054104 (2009).
[10] T. H. Dunning Jr, The Journal of chemical physics **90**, 1007–1023 (1989).
[11] H.-J. Werner, P. Knowles, G. Knizia, F. Manby, M. Schütz, P. Celani, T. Korona, R. Lindh, A. Mitrushenkov, G. Rauhut, *et al.*, See http://www. molpro. net (2010).
[12] S. F. Boys and F. d. Bernardi, Molecular Physics **19**, 553–566 (1970).
[13] A. D. Buckingham, (Wiley, New York, 1978).
[14] T. Korona and H.-J. Werner, J. Chem. Phys. **118**, 3006 (2003).
[15] C. C. J. H. D. Cohen, J. Chem. Phys. **43**, S34–S39 (1965).
[16] D. Ndaw, C. T. Bop, G. Dieye, N. A. B. Faye, and F. Lique, Monthly Notices of the Royal Astronomical Society **503**, 5976–5983 (2021).
[17] M. Lanza, Y. Kalugina, L. Wiesenfeld, A. Faure, and F. Lique, Monthly Notices of the Royal Astronomical Society **443**, 3351–3358 (2014).
[18] S. Green, The Journal of Chemical Physics **62**, 2271–2277 (1975).
[19] J. Hutson and S. Green, Collaborative computational project (1994).
[20] M. H. Alexander and D. E. Manolopoulos, The Journal of chemical physics **86**, 2044–2050 (1987).
[21] C. T. Bop, F. Lique, A. Faure, E. Quintas-Sánchez, and R. Dawes, Monthly Notices of the Royal Astronomical Society **501**, 1911–1919 (2020), https://academic.oup.com/mnras/article-pdf/501/2/1911/35335662/staa3821.pdf.
[22] B. Desrousseaux, E. Quintas-Sánchez, R. Dawes, and F. Lique, The Journal of Physical Chemistry A **123**, 9637–9643 (2019).
[23] O. Denis-Alpizar, E. Quintas-Sánchez, and R. Dawes, Monthly Notices of the Royal Astronomical Society **512**, 5546–5551 (2022).
[24] A. Spielfiedel, M. L. Senent, Y. Kalugina, Y. Scribano, C. Balança, F. Lique, and N. Feautrier, The Journal of Chemical Physics **143**, 024301 (2015).
[25] F. Lique, A. Spielfiedel, and J. Cernicharo, Astronomy and Astrophysics **451**, 1125–1132 (2006).
[26] P. Hily-Blant, G. Pineau des Forêts, A. Faure, and F. Lique, arXiv e-prints , arXiv–2112 (2021).
[27] M. Asplund, N. Grevesse, and A. Sauval, Communications in Asteroseismology **147**, 76–79 (2006).
[28] D. Neufeld, B. Godard, M. Gerin, G. P. Des Forêts, C. Bernier, E. Falgarone, U. Graf, R. Güsten, E. Herbst, P. Lesaffre, *et al.*, Astronomy & Astrophysics **577**, A49 (2015).
[29] V. Wakelam, P. Caselli, C. Ceccarelli, E. Herbst, and A. Castets, Astronomy & Astrophysics **422**, 159–169 (2004).
[30] J. Goicoechea, J. Pety, M. Gerin, D. Teyssier, E. Roueff, P. Hily-Blant, and S. Baek, Astronomy & Astrophysics **456**, 565–580 (2006).
[31] C. Vastel, D. Quénard, R. Le Gal, V. Wakelam, A. Andrianasolo, P. Caselli, T. Vidal, C. Ceccarelli, B. Lefloch, and R. Bachiller, Monthly Notices of the Royal Astronomical Society **478**, 5514–5532 (2018).
[32] A. Fuente, J. R. Goicoechea, J. Pety, R. Le Gal, R. Martín-Doménech, P. Gratier, V. Guzmán, E. Roueff, J. C. Loison, G. M. M. Caro, *et al.*, The Astrophysical Journal Letters **851**, L49 (2017).
[33] O. Denis-Alpizar and J. Rubayo-Soneira, Monthly Notices of the Royal Astronomical Society **486**, 1255–1259 (2019).